

# Electrostatically induced phase transitions in superconducting complex oxides

Li Han and C. A. R. Sá de Melo

*School of Physics, Georgia Institute of Technology, Atlanta, Georgia 30332, USA*

(Dated: February 6, 2020)

We describe quantum phase transitions in superconducting complex oxides which could be tuned by electrostatic charge transfer. Using a simple model for the superconductivity of a thin film or surface of a bulk copper oxide, we show that tuning the carrier density may allow the visitation of several superconducting phases with different pairing symmetries such as extended  $s$ - ( $se$ ),  $d$ - and ( $se \pm id$ )-wave. We construct a universal phase diagram for single-band superconductors with  $se$ - and  $d$ -wave components of the order parameter based on symmetry considerations alone. For a specific model with nearest neighbor attraction, we obtain the phase diagram in the interaction versus filling factor space showing the boundaries of the possible phases. Finally, we calculate the superfluid density and penetration depth as characteristic properties of each phase.

PACS numbers: 74.78.-w, 74.78.Bz, 74.62.-c, 74.62.Dh

Substantial progress in tuning carrier density has been achieved recently in systems like amorphous Bismuth, where a superconducting-insulator transition was driven by electrostatic fields<sup>1</sup>. This experimental realization has opened the possibility of studying quantum phase transitions by tuning carrier density electrostatically. Several groups are currently attempting the use of electrostatic doping to control the carrier density in complex oxides, with particular attention to cuprate superconductors. The phase diagram of cuprate superconductors as a function of chemical substitution (oxygen deficiency) is known for Lanthanum (Yttrium) cuprates, but as it is well documented in the literature that the relation between chemical doping or oxygen deficiency to carrier density is very complicated<sup>2</sup>.

Electrostatic doping has substantial advantages over chemical doping, as the carrier density can be tuned continuously and does not produce undesired effects such as disorder or changes in the crystal structure as chemical doping or oxygen deficiency often does. The method when applied to cuprates should be able to answer the long standing question of what really is the phase diagram of the system as a function of carrier density, and to clarify the origin of the dome that reflects an optimally doped superconductor with the highest critical temperature. In particular, if the results of electrostatic doping are substantially different from those of chemical doping, showing for instance that the critical temperature continues to grow beyond the expected optimal chemical doping point, then it could be directly inferred that chemical doping does introduce undesired effects.

Although electrostatic doping has remarkable advantages over chemical doping, its use is limited to thin films and the surface of bulk systems. However, it is probably the best way to study the dependence of physical properties of complex oxides and other materials on carrier density. Furthermore, from the point of view of devices, the electrostatic tuning of the phase diagram at fixed temperature would be extremely useful to produce a superconducting switch, as the resistance of a thin film could be turned on and off via a gate voltage.

It is in anticipation of these exciting experiments currently underway in several labs around the world, that we describe the possibility of using electrostatic tuning of carrier density to study quantum phase transitions in complex oxides. As an example we chose to study a simple model of complex oxides representing a cuprate superconductor. We model such a system via an extended attractive Hubbard model in a two-dimensional lattice, and derive the universal phase diagram when only two pure order parameter symmetries are allowed. Based on symmetry alone there are several possibilities: pure extended  $s$ - ( $se$ ) and  $d$ -wave phases, and ( $se \pm d$ ) phases that do not break time-reversal symmetry and ( $se \pm id$ ) phases that do. For a specific model where only nearest neighbor attraction is included, the  $se$ -wave phase dominates at lower filling factor, while the  $d$ -wave solution dominates at higher filling factor, with a ( $se \pm id$ )-wave phase in between, whereas the ( $se \pm d$ )-wave is not accessible. The phase diagram for such a minimal model is very rich, and the existence of various phases as a function of filling factor for fixed interactions can be tested via measurements of the penetration depth (superfluid density) at low temperatures.

To study the physics discussed above we start from a two-dimensional hamiltonian

$$H = -t \sum_{\langle ij \rangle \sigma} c_{i\sigma}^\dagger c_{j\sigma} - U \sum_i n_{i\uparrow} n_{i\downarrow} - V \sum_{\langle ij \rangle \sigma \sigma'} n_{i\sigma} n_{j\sigma'} \quad (1)$$

describing thin films or the surface layer of a bulk cuprate on a square lattice. Here, the local particle number operator is  $n_{i\sigma} = c_{i\sigma}^\dagger c_{i\sigma}$ , while  $-U$  and  $-V$  correspond to on-site and nearest neighbor attractions, respectively.

In order to establish the quantum phases as a function of carrier density, we start by constructing the partition function  $Z = \int \mathcal{D}c^\dagger \mathcal{D}c e^S$  for the action

$$S = \int_0^\beta d\tau \left[ \sum_{i\sigma} c_{i\sigma}^\dagger(\tau) (-\partial_\tau + \mu) c_{i\sigma}(\tau) - H(c^\dagger, c) \right] \quad (2)$$

Introducing order parameters for local  $s$ -wave  $\tilde{\Delta}_{sl}$ , extended  $s$ -wave  $\tilde{\Delta}_{se}$  and  $d$ -wave  $\tilde{\Delta}_d$  pairing, we can write

the action as

$$S = -\frac{N_s}{T} \sum_{q,\alpha} \frac{|\tilde{\Delta}_\alpha(q)|^2}{V_\alpha} + \text{Tr} \ln \left( \frac{\mathbf{G}_0^{-1}}{T} - \frac{\mathbf{V}}{T} \right) + \frac{\mu N_s}{T}, \quad (3)$$

where  $\alpha = sl, se, d$ ; the interactions are  $V_{sl} = U$ ,  $V_{se} = V_d = V$ ; and the four-vector  $q = (i\nu_n, \mathbf{q})$ .

The inverse free fermion propagator matrix is

$$\mathbf{G}_0^{-1}(k, k') = \begin{pmatrix} i\omega_n - \xi_{\mathbf{k}} & 0 \\ 0 & i\omega_n + \xi_{\mathbf{k}} \end{pmatrix} \delta_{k,k'} \quad (4)$$

with kinetic energy  $\xi_{\mathbf{k}} = \epsilon_{\mathbf{k}} - \mu$ , band dispersion  $\epsilon_{\mathbf{k}} = -2t [\cos(k_x a) + \cos(k_y a)]$ , chemical potential  $\mu$ , four-vector  $k = (i\omega_n, \mathbf{k})$ , and unit cell length  $a$ . The additional matrix appearing in Eq. (3) is

$$\mathbf{V}(k, k') = \begin{pmatrix} 0 & \tilde{\Delta}_\alpha(k - k') \\ \tilde{\Delta}_\alpha^*(-k + k') & 0 \end{pmatrix} \lambda_\alpha(\mathbf{k}, \mathbf{k}'), \quad (5)$$

where the Einstein summation over  $\alpha$  is understood, and  $\lambda_\alpha(\mathbf{k}, \mathbf{k}')$  are the symmetry factors for the order parameters, which in the limit of zero momentum pairing ( $\mathbf{k} = \mathbf{k}'$ ) become  $\lambda_{sl}(\mathbf{k}, \mathbf{k}) = 1$ ,  $\lambda_{se}(\mathbf{k}, \mathbf{k}) = \cos(k_x a) + \cos(k_y a)$ ,  $\lambda_d(\mathbf{k}, \mathbf{k}) = \cos(k_x a) - \cos(k_y a)$ .

The saddle point approximation gives qualitatively correct results either at low temperatures ( $T \ll T_c$ ) for any interaction strength or for weak interactions  $V \ll bw = 8t$  at any temperature<sup>3,4</sup>, where  $bw$  is the bandwidth in two-dimensions. In these cases, the effective action can be approximated by

$$S = -\frac{N_s}{UT} |\tilde{\Delta}_{sl}|^2 - \frac{N_s}{VT} (|\tilde{\Delta}_{se}|^2 + |\tilde{\Delta}_d|^2) + S_2 + \frac{\mu N_s}{T}. \quad (6)$$

The second term in the action  $S_2 = \sum_{\mathbf{k}, \gamma} \ln [1 + \exp(-E_{\mathbf{k}, \gamma}/T)]$ , contains the quasi-particle ( $\gamma = 2$ ) or quasihole ( $\gamma = 1$ ) energies  $E_{\mathbf{k}, \gamma} = (-)^{\gamma} \sqrt{\xi_{\mathbf{k}}^2 + |\tilde{\Delta}_\alpha \lambda_\alpha(\mathbf{k})|^2}$ , where the symmetry function is defined as  $\lambda_\alpha(\mathbf{k}) = \lambda_\alpha(\mathbf{k}, \mathbf{k})$ .

Notice that even in such a simple model with local ( $-U$ ) and nearest neighbor ( $-V$ ) attractions the number of possible phases is quite large. There are three possible pure phases: local  $s$ -wave ( $sl$ ); extended  $s$ -wave ( $se$ ) and  $d$ -wave ( $d$ ). There are several possible binary mixed phases  $sl \pm se$ ,  $sl \pm d$ , and  $se \pm d$ , which do not break time-reversal symmetry, as well as those that do like  $sl \pm ise$ ,  $sl \pm id$ , and  $se \pm id$ . Lastly there are also several ternary mixed phases involving all three symmetries  $sl$ ,  $se$ , and  $d$ . Since the situation is quite complicated in the more general case, for clarity and simplicity, we study here the case of  $U = 0$ , which allows for solutions involving only  $se$ - and  $d$ -wave symmetries. In this simpler case there are only six possible phases. The pure phases are  $se$  and  $d$ . The mixed phases are  $se \pm d$ , and  $se \pm id$ . Thus, from now on, we will confine ourselves to this simpler analysis. In this case, the order parameter equations can be obtained by minimizing the action  $S$  through the conditions  $\delta S / \delta \tilde{\Delta}_{se}^* = 0$  and  $\delta S / \delta \tilde{\Delta}_d^* = 0$ .

For the  $se$ -wave component of the order parameter the first condition leads to

$$\tilde{\Delta}_{se} = \frac{V}{N_s} \sum_{\mathbf{k}} \frac{\tanh(E_{\mathbf{k},2}/2T)}{2E_{\mathbf{k},2}} \Lambda_{se}(\mathbf{k}), \quad (7)$$

where  $\Lambda_{se}(\mathbf{k}) = \tilde{\Delta}_{se} [\lambda_{se}(\mathbf{k})]^2 + \tilde{\Delta}_d \lambda_{se}(\mathbf{k}) \lambda_d(\mathbf{k})$ . Correspondingly for the  $d$ -wave component

$$\tilde{\Delta}_d = \frac{V}{N_s} \sum_{\mathbf{k}} \frac{\tanh(E_{\mathbf{k},2}/2T)}{2E_{\mathbf{k},2}} \Lambda_d(\mathbf{k}), \quad (8)$$

where  $\Lambda_d(\mathbf{k}) = \tilde{\Delta}_d [\lambda_d(\mathbf{k})]^2 + \tilde{\Delta}_{se} \lambda_{se}(\mathbf{k}) \lambda_d(\mathbf{k})$ .

The number equation that fixes the chemical potential is obtained through the thermodynamic relation  $N = -\partial \Omega / \partial \mu$ , where  $\Omega = -T \ln Z$  is the thermodynamic potential. In the present approximation the thermodynamic potential is  $\Omega = -TS$ , and the number equation reduces to

$$\nu = \frac{1}{N_s} \sum_{\mathbf{k}} \left[ 1 - \frac{\xi_{\mathbf{k}}}{E_{\mathbf{k},2}} \tanh(E_{\mathbf{k},2}/2T) \right], \quad (9)$$

where  $\nu = N/N_s$  is the filling factor.

The phase difference between the  $s$ -wave and  $d$ -wave components of the order parameter is defined to be  $\delta\phi = \phi_d - \phi_{se}$ , where  $\phi_d$  is the phase of the  $d$ -wave order parameter  $\tilde{\Delta}_d = |\tilde{\Delta}_d| e^{i\phi_d}$  and  $\phi_{se}$  is the phase of the  $s$ -wave order parameter  $\tilde{\Delta}_{se} = |\tilde{\Delta}_{se}| e^{i\phi_{se}}$ . Simultaneous solutions of Eqs. (7), (8), and (9) reduce to saddle-point solutions of  $\Omega$  only for  $\delta\phi = \pi/2, 3\pi/2$  which correspond to  $se \pm id$  phases that break time-reversal symmetry, and  $\delta\phi = 0, \pi$  which correspond to  $se \pm d$  phases that do not.

The saddle point critical temperature can be obtained by setting the order parameters  $\tilde{\Delta}_{se} = 0$  and  $\tilde{\Delta}_d = 0$  in Eqs. (7), (8), and (9). In this case, the filling factor dependence of critical temperature  $T_c(\nu)$  and critical chemical potential  $\mu_c(\nu)$  can be obtained for pure  $se$ - and  $d$ -wave symmetries. The solutions for  $T_c(\nu)$  are shown in Fig. 1 for  $V/t = 3.0$ . Notice that the  $s$ -wave phase is favored at lower filling factors, while the  $d$ -wave phase is favored at higher filling factors. In addition, the critical temperature is symmetric about  $\nu = 1$ , since the Helmholtz free energy  $F = \Omega + \mu N$  is invariant under the transformation  $\mu \rightarrow -\mu$  and  $\nu \rightarrow 2 - \nu$ .

In order to construct a universal phase diagram for all possible phases it is important to construct the Ginzburg-Landau theory near  $T_c$  by expanding the action described in Eq. (6) in terms of the order parameters  $\tilde{\Delta}_{se}$ ,  $\tilde{\Delta}_d$  and their complex conjugates. From the thermodynamic potential  $\Omega = -TS$ , we can calculate the Helmholtz free energy  $F = \Omega + \mu N$ . The free energy per site  $\mathcal{F} = F/N_s$  takes the simple form

$$\mathcal{F} = a_{se} |\tilde{\Delta}_{se}|^2 + a_d |\tilde{\Delta}_d|^2 + b_{se} |\tilde{\Delta}_{se}|^4 + b_d |\tilde{\Delta}_d|^4 + 2b_{sd} \left[ 1 + \frac{1}{2} \cos(2\delta\phi) \right] |\tilde{\Delta}_{se}|^2 |\tilde{\Delta}_d|^2 + \mu(\nu - 1). \quad (10)$$

This expression has precisely the expected form, based on symmetry grounds alone, when paring with  $se$ - and

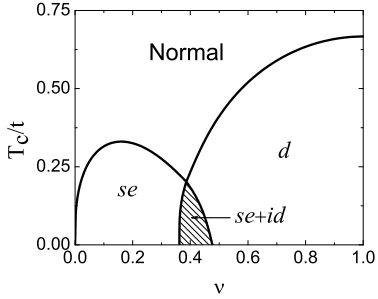


FIG. 1: Plots of the critical temperature  $T_c$  as a function of filling factor  $\nu$  at fixed interaction ( $V/t = 3.0$ ), showing the the  $se$ -,  $d$ -, and  $(se + id)$ -wave phases. Notice the tetracritical point where the normal and all superconducting phases meet.

$d$ -wave components are possible. However, the coefficients  $a$  and  $b$  depend explicitly on the parameters of the microscopic model used. For the construction of the universal phase diagram we introduce the dimensionless parameters  $X = \{b_{sd} [1 + \frac{1}{2} \cos(2\delta\phi)] / b_d\} \times |a_d/a_{se}|$ , and  $Y = (b_{se}/b_d) \times |a_d/a_{se}|^2$ . Minimization of the free energy in Eq. (10) and a stability analysis leads to the universal phase diagram shown in Fig. 2, where all possible phases ( $se$ ,  $d$ ,  $se \pm d$  and  $se \pm id$ ) are indicated. Notice that the free energy depends only on  $2\delta\phi$  and does not distinguish between the phases  $se + d$  and  $se - d$ , which are thus degenerate. The same applies to the phases  $se + id$  and  $se - id$ , which are also degenerate. In the particular case of  $se \pm id$  phases, time-reversal symmetry is broken while chirality is not, the latter of which requires additional terms in the free energy for the distinction between the  $se + id$  and  $se - id$  phases. Notice that a tetracritical point occurs at  $Y = X = 1$ , where the normal and superconducting phases with  $se$ ,  $d$  and  $se \pm id$  symmetries meet.

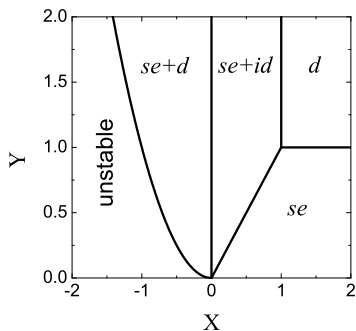


FIG. 2: Universal phase diagram for superconductors exhibiting order parameters with  $se$ - and  $d$ -wave components is shown, in the space of the dimensionless parameters  $X = \{b_{sd} [1 + \frac{1}{2} \cos(2\delta\phi)] / b_d\} \times |a_d/a_{se}|$  and  $Y = (b_{se}/b_d) \times |a_d/a_{se}|^2$ . Depending on microscopic details, different regions of the phase diagram are accessible.

For the specific microscopic model discussed above the

variable  $X$  is always positive, such that the system is always stable and the  $se \pm d$  phases are not accessible. Thus, we elaborate further only on the accessible phases  $se$ ,  $d$ , and  $se \pm id$ . At low temperatures  $T \ll T_c$ , the Helmholtz free energy per site can be approximated by

$$\mathcal{F} = \frac{1}{V} \sum_{\alpha} |\tilde{\Delta}_{\alpha}|^2 - \frac{T}{N_s} \sum_{\mathbf{k}, \gamma} \ln [1 + \exp(-E_{\mathbf{k}, \gamma}/T)] + \mu(\nu - 1)$$

for any interaction strength  $V/t$ . A comparison of the free energies for all the accessible phases produces the phase diagram in the interaction ( $V/t$ ) versus filling factor ( $\nu$ ) space shown in Fig. 3. Notice that pure  $se$  and  $d$  phases are always separated by  $(se \pm id)$  phases, and their phase boundaries describe continuous transitions. For weak attractions the region of filling factors where  $(se \pm id)$  phase is realized is very narrow. However, the region increases substantially as the interaction  $V/t$  gets larger. For instance when  $V/t = 3.0$ , the  $(se \pm id)$  phase exists between  $\nu_{min} \approx 0.36$  and  $\nu_{max} \approx 0.48$ .

We had hoped that a topological quantum phase transition<sup>5</sup> characterized by the emergence of a gapful  $d$ -wave superconductor from a gapless  $d$ -wave superconductor would also emerge within the  $d$ -wave region of the phase diagram. However, within the  $d$ -wave boundary the chemical potential always fall inside the band limits ( $|\mu| < 4t$ ), and one can always find zeros of the quasiparticle excitation spectrum given by  $E_{\mathbf{k}, 2} = 0$ . However, the transition from  $d$ - to  $(se \pm id)$ -wave is also very exotic as it involves a change in the excitation spectrum from gapless to fully gapped with a corresponding change in topology of the quasiparticle-quasihole excitation manifold, and a change in order parameter symmetry accompanied by the spontaneous breaking of time-reversal.

Since in standard condensed matter physics the interactions in the same material can not be tunned, one can hope to visit different phases by changing the temperature or tuning the filling factor (carrier density)<sup>6</sup>. If the tuning of carrier density via electrostatic means can be achieved experimentally for complex oxides, then quantum phase transitions may be studied as a function of filling factor<sup>2</sup>. Since electrostatic tuning of carrier density can only be implemented in thin films or at the surface of bulk materials, additional experiments to characterize the various phases are difficult. However, in such geometry, measurements of the penetration depth  $\lambda(\nu, T)$  may be possible. Given that  $\lambda(\nu, T) \propto \rho^{-2}(\nu, T)$ , where  $\rho(\nu, T)$  is the superfluid density, then a distinguished low-temperature behavior varying from a linear increase with temperature in the  $d$ -wave phase to an exponentially activated behavior in the  $se$ -wave phase could be revealed as the filling factor  $\nu$  is varied.

In order to describe the behavior of  $\lambda(\nu, T)$ , we calculate the superfluid density tensor

$$\rho_{ij}(\nu, T) = \frac{1}{L^2} \sum_{\mathbf{k}} [2n_{\mathbf{k}} \partial_i \partial_j \xi_{\mathbf{k}} - Y_{\mathbf{k}} \partial_i \xi_{\mathbf{k}} \partial_j \xi_{\mathbf{k}}], \quad (11)$$

at low  $T$ , where  $n_{\mathbf{k}} = (1/2) [1 - \xi_{\mathbf{k}} \tanh(E_{\mathbf{k}, 2}/2T)/E_{\mathbf{k}, 2}]$  is the momentum distribution, and  $Y_{\mathbf{k}} =$

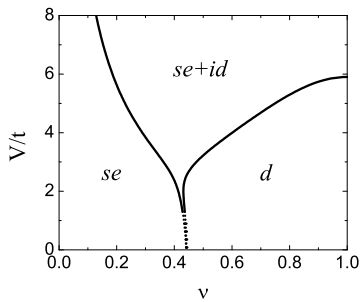


FIG. 3: The zero-temperature phase diagram in the interaction  $V/t$  versus filling factor  $\nu$  plane showing the boundaries between all accessible phases  $se$ ,  $d$ , and  $se + id$  for the microscopic model discussed. The phase transitions are always continuous across the boundaries.

$(2T)^{-1}\text{sech}^2(E_{\mathbf{k},2}/2T)$  is the Yoshida function. Notice that  $\rho_{xx} = \rho_{yy}$  and  $\rho_{xy} = \rho_{yx}$  for all order parameter symmetries. In Fig. 4, we show the temperature dependence of the superfluid density in the  $se$ -,  $(se \pm id)$ -, and  $d$ -wave phases. At low temperatures, the superfluid density for the  $se$ -wave phase exhibits an exponentially activated behavior  $\rho_{se}(0) - \rho_{se}(T) \sim \exp(-|\tilde{\Delta}_{se}|/T)$ , due to the presence of full gap in the quasiparticle excitation spectrum  $E_{\mathbf{k},2}$ , with similar behavior for the  $(se \pm id)$  phase. However, in the  $d$ -wave case the superfluid density decreases linearly with temperature  $\rho_d(0) - \rho_d(T) \sim T$ , as expected from the nodal structure of  $E_{\mathbf{k},2}$ .

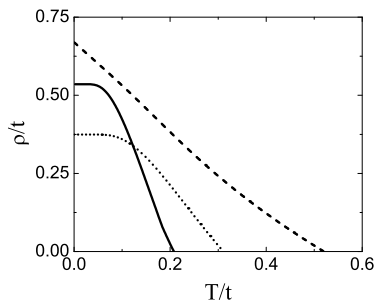


FIG. 4: The superfluid density  $\rho/t$  versus temperature  $T/t$  at fixed interaction  $V/t = 3.0$ . The dotted line corresponds to  $se$ -wave for  $\nu = 0.24$ , the solid line to  $(se \pm id)$ -wave for  $\nu = 0.38$ , and the dashed line to  $d$ -wave for  $\nu = 0.60$ .

Before concluding, we would like to make an important remark. For the model described here there is no antiferromagnetic phase near half-filling. This phase emerges by replacing the on-site attractive- $U$  term by an on-site repulsive (Hubbard- $U$ ) term in the Hamiltonian of Eq. (1). The full solution of the problem including the on-site repulsion  $U$ , and the nearest neighbor attraction ( $-V$ ) is quite complex, however one can make a few qualitative statements for  $U/t \gg V/t$  and fixed  $V/t$ . In this case, the system is an antiferromagnetic insulator at and near half-filling ( $\nu = 1$ ), however away from it the effects of a locally repulsive term are dramatically reduced and with decreasing filling factor superconductivity is achieved first for the  $d$ -wave phase, then for the mixed phase ( $se \pm id$ ) and finally for the  $se$ -wave phase. Since the change in symmetry of the order parameter from  $d$ - to mixed phase to  $se$ -wave occurs reasonably far away from half-filling, such a transition is not dramatically affected by  $U$ . Thus, even in more realistic models for complex oxides such as the cuprates, the transition proposed here should persist at lower filling factors.

We have discussed a simple extended attractive Hubbard model to describe single-band complex oxide superconductors in two-dimensions, where the filling factor can be adjusted via electrostatic doping. Based on symmetry alone, we established that the possible superconducting states are extended  $s$ -wave ( $se$ ),  $d$ -wave ( $d$ ) and mixed phases which break  $(se \pm id)$  and do not break  $(se \pm d)$  time-reversal symmetry. However, we found that only the  $se$ -,  $d$ - and  $(se \pm id)$  phases are accessible within a nearest neighbor attraction model, and that there exists a tetracritical point where the normal and all superconducting phases meet at finite temperature. We have shown that quantum phase transitions between various superconducting phases take place at filling factors far from half-filling, and analysed the temperature dependence of the superfluid density (penetration depth) near the boundaries of such transitions, where the characteristic power law behavior of the  $d$ -wave symmetry is replaced by the exponentially activated behavior of the  $se$ -wave symmetry.

#### Acknowledgments

We thank Allen Goldman for discussions and NSF (DMR-0709584) for support.

<sup>1</sup> K. A. Parendo et al. Phys. Rev. Lett. **94**, 197004 (2005).

<sup>2</sup> C. H. Ahn et al., Rev. Mod. Phys. **78**, 1185 (2006).

<sup>3</sup> P. Nozières and S. Schmitt-Rink, J. Low Temp. Phys. **59**, 195 (1985).

<sup>4</sup> M. Iskin and C. A. R. Sá de Melo, Phys. Rev. B **72**, 224513 (2005).

<sup>5</sup> R. D. Duncan and C. A. R. Sá de Melo, Phys. Rev. B **62**, 9675 (2000).

<sup>6</sup> K. A. Parendo, K. H. Sarwa B. Tan, and A. M. Goldman, Phys. Rev. B **73**, 174527 (2006).